Modeling Multiscale-Multiphase-Multicomponent Subsurface Reactive Flows using Advanced Computing

P. Lichtner[α] (PI: lichtner@lanl.gov), C. Lu[α], B. Philip[α], D. Moulton[α], G. Hammond[β], S. Yabusaki[β], R. Mills[γ], B. Smith[δ], A. Valocchi[ϵ]

[α]Los Alamos National Laboratory,[β]Pacific Northwest National Laboratory,[γ]Oak Ridge National Laboratory,[δ]Argonne National Laboratory,[ϵ]University of Illinois at Urbana-Champaign

1. Introduction

- Predictive modeling of subsurface reactive flows is a daunting task because of the wide range of spatial scales involved—from the pore to the field scale—ranging over more than six orders of magnitude, and the wide range of time scales involved from seconds or less to millions of years.
- Failures of simple K_d–type models are common place, for example, simulations of the fate of uranium in the 300 Area at Hanford using a K_d model predicted that uranium would be removed by ambient groundwater flow within a decade. Fifteen years later the uranium plume remains where it was with no apparent measurable migration (Zachara et al., 2005), caused by slow leaching of uranium from millimeter or smaller scales.
- Capturing the extreme range of scales (1 mm – 100 m) is impossible with current and near-future computing capabilities employing conventional single continuum models with simple orthogonal grids. For example, discretizing a computational domain measuring 2 km $\times$ 1 km $\times$ 500 m = 10^9 m^3, into cubic millimeter nodes would require 10^{18} computational nodes to describe.
- Two promising approaches to solve this problem are to apply grid refinement only where needed using adaptive mesh refinement (AMR) techniques, and incorporate a sub-grid scale model that can account for millimeter scales into the primary-grid continuum model.

2. Code Enhancements Planned in SciDAC II Project

2.1 Modeling Multiscale Processes

- Represent system through multiple interacting continua with a single primary continuum coupled to sub-grid scale secondary continua (Lichtner and Kang, 2007)
- Associate sub-grid scale model with node in primary continuum
  - 1D computational domain
  - Multiple sub-grid models may be associated with a subset of primary continuum nodes
  - Degrees of freedom: $N \times N_K \times N_{\rm DCM} \times N_C$
  - N–number of primary continuum nodes
  - N_K–sub-grid classes
  - $N_{\rm DCM}$–number of nodes to discretized sub-grid continuum
  - N_c–number of chemical components

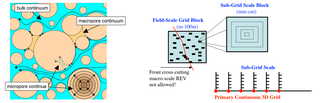

Figure 1: *Schematic illustration of multiscale processes in a heterogeneous porous medium and primary and secondary continua with connectivity of sub-grid scale model.*

2.2 Adaptive Mesh Refinement

- AMR provides front tracking capability in the primary grid that can range from centimeter to tens of meters.
- Disparate length scales can be effectively addressed using AMR by introducing local fine resolution only in regions where needed. This can significantly reduce memory and computational costs for simulating complex physical processes exhibiting localized fine scale features that need to be resolved.
- Sub-grid scale models can be introduced in regions of significant activity and not at every node within the 3D domain. As demonstrated below, it is not necessary to include the sub-grid model equations in the primary continuum Jacobian even though these equations are solved in a fully coupled manner.

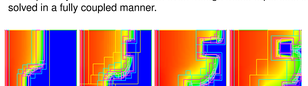

Figure 2: *Example of AMR using SAMRAI, an object oriented C++ software framework providing support for massively parallel adaptive mesh refinement multiphysics applications (Pernice and Philip, 2006).*

- AMR capabilities are provided by SAMRAI (Structured Adaptive Mesh Refinement Application Infrastructure) provides:
  - parallel load balancing
  - geometry
  - inter-level and intra-level communication
  - different data centerings- vertex, cell, edge ..
  - regridding
  - basic mathematical operations
  - solver interfaces to PETSc
- Using SAMRAI with application codes written in F90 requires implementation of a portable C++–F90 interface (Wang et al., 2004).

2.3 Unstructured Grids with PETSc Sieve Objects

- To capture irregular geology and enable local regions of fixed grid refinement, we will introduce an unstructured grid capability within our PFLOTRAN code's integral finite volume formulation.
- PFLOTRAN has been written with this eventuality in mind:
  - Fluxes calculated by looping over all connections between nodes.
  - Non-Cartesian meshes are easily substituted using a PETSc DM.
- PETSc DA objects to manage data distribution on a Cartesian mesh.
- The Mesh class is an reformulation of the DA for arbitrary topology (Knepley and Karpeev, 2005).
  - Sieves, discrete topological objects, represent the computational mesh in terms of a *covering* relation.
  - Mesh topology is cleanly separated from geometry and other fields (e.g., temperature, pressure, saturation, ...).
  - Only local physics routines need geometry information.
  - Greatly simplifies data movement and repartitioning.
- The Mesh, like the DA, manages the parallel data structures.
- No substantial changes to the PFLOTRAN code are required.
- The Mesh, through a DM, can also manage a multilevel solver.

2.4 Upscaling

- Upscaling and AMR go hand-in-hand: as the grid is refined or coarsened, material properties such as permeability must be calculated at the new scale.

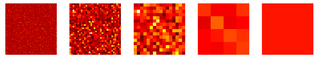

Figure 3: *A fine-scale realization* (128×128) *of a random permeability field,* $\kappa(x,y) = \zeta^{-\ln(\alpha)}$*,*$\zeta$ *uniformly distributed in* $(0,1)$*, with* $\alpha = 5$ *(left) is followed by successively upscaled fields (*$N \times N$ *with* $N = 32, 16, 4,$ *and* 1*) obtained with Multigrid Homogenization (Moulton et al., 1998).*

- *Coarse-Scale Anisotropy*: permeability must, in general, be considered as a tensor at larger scales even if it is a scalar (i.e., isotropic) at the finest scale.

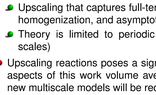

① Uniform flow from left to right is governed by the harmonic mean.

② Uniform flow from bottom to top is governed by the arithmetic mean.

③ This suggests a diagonal permeability tensor is sufficient, however, if the stripes are not aligned with the coordinate axes this equivalent permeability is described by a full tensor.

- A single multi-dimensional average is inadequate for modeling flow (MacLachlan and Moulton, 2006)
- Upscaling that captures full-tensor permeability includes multigrid homogenization, and asymptotic theory for periodic media.
- Theory is limited to periodic two-scale media (well separated scales)
- Upscaling reactions poses a significant challenge as well. In some aspects of this work volume averaging will suffice, while in others new multiscale models will be required.

2.5 Software Management and Development

PFLOTRAN leverages several open source packages:

- Mercurial is used for revision control (`http://www.selenic.com/mercurial/wiki/`)
- Trac is used for project management (`http://trac.edgewall.com/`)
- Plone is used for content management (`http://plone.org`) for the public web site
- Open source releases will be posted on the public web site (`http://software.lanl.gov/pflotran/`)

3. The Massively Parallel Reactive Flow and Transport Code PFLOTRAN

- The computer code PFLOTRAN solves a coupled system of mass and energy conservation equations for a number of phases including H_2O, supercritical CO_2, and black oil, and a gaseous phase. PFLOTRAN describes coupled thermal-hydrologic-chemical (THC) processes in variably saturated, nonisothermal, porous media in one (1D), two (2D), or three (3D) spatial dimensions.
- The multiphase partial differential equations solved by PFLOW for mass and energy conservation can be summarized as (Lichtner et al., 1996):

$$\frac{\partial}{\partial t}\left(\phi \sum_\alpha s_\alpha \rho_\alpha X_i^\alpha\right) + \nabla\cdot\sum_\alpha\left[\boldsymbol{q}_\alpha \rho_\alpha X_i^\alpha - \phi s_\alpha D_\alpha \rho_\alpha \nabla X_i^\alpha\right] = Q_i^\alpha, \quad (1a)$$

$$\frac{\partial}{\partial t}\left(\phi \sum_\alpha s_\alpha \rho_\alpha U_\alpha + (1-\phi)\rho_r c_r T\right) + \nabla\cdot\left[\boldsymbol{q}_\alpha \rho_\alpha H_\alpha - \kappa \nabla T\right] = Q_e. \quad (1b)$$

In these equations, α designates a phase (e.g. H_2O, supercritical CO_2, g), species are designated by the subscript i (e.g. $w = H_2O$, $c = CO_2$), ϕ denotes porosity of the geologic formation, s_α denotes the saturation state of the phase; X_i^α denotes the mole fraction of species i; ρ_α, H_α, U_α refer to the molar density, enthalpy, and internal energy of each fluid phase, respectively; $\boldsymbol{q}_\alpha$ denotes the Darcy flow rate defined by

$$\boldsymbol{q}_\alpha = -\frac{k k_{r_\alpha}}{\mu_\alpha}\nabla(p_\alpha - W_\alpha \rho_\alpha g \boldsymbol{z}), \quad (2)$$

where k refers to the water saturated permeability, k_{r_α} denotes the relative permeability, μ_α denotes the fluid viscosity, W_α denotes the formula weight, and g denotes the acceleration of gravity. The source/sink terms Q_i^α and Q_e, describe injection and extraction at wells.

- The multicomponent reactive transport equations solved by PTRAN have the form (Lichtner et al., 1996):

$$\frac{\partial}{\partial t}\left(\phi \sum_\alpha s_\alpha \Psi_j^\alpha\right) + \nabla\cdot\sum_\alpha \boldsymbol{\Omega}_j^\alpha = -\sum_m \nu_{jm} I_m, \quad (3)$$

for the jth primary species, and

$$\frac{\partial \phi_m}{\partial t} = \overline{V}_m I_m, \quad (4)$$

for the mth mineral.

- Definitions: Ψ_j^α, $\boldsymbol{\Omega}_j^\alpha$ denote the total concentration and flux, defined by the expressions

$$\Psi_j^\alpha = \delta_{\alpha l} C_j^\alpha + \sum_i \nu_{ji} C_i^\alpha, \quad (5)$$

and

$$\boldsymbol{\Omega}_j^\alpha = (-\tau\phi s_\alpha D_\alpha \nabla + \boldsymbol{q}_\alpha)\Psi_j^\alpha, \quad (6)$$

where C_j^α denotes the solute concentration in phase α, C_i^α denotes the concentration of the ith secondary species related to the concentration of primary species through the mass action equations

$$C_i^\alpha = (\gamma_i^\alpha)^{-1} K_i^\alpha \prod_j \left(\gamma_j^\alpha C_j^\alpha\right)^{\nu_{ji}}, \quad (7)$$

where γ_j^α denotes the activity coefficient, K_i^α the equilibrium constant for reaction (10).

- The mineral concentration is represented by the volume fraction ϕ_m with molar volume $\overline{V}_m$. The kinetic reaction rate I_m for the mth mineral is assumed to have the form

$$I_m = -k_m A_m \Phi(\phi_m)\left(1 - K_m Q_m\right), \quad (8)$$

based on transition state theory, where k_m denotes the kinetic rate constant, K_m the equilibrium constant for reaction (11), A_m the mineral specific surface area, and Q_m the ion activity product defined by

$$Q_m = \prod_j \left(\gamma_j^\alpha C_j^\alpha\right)^{\nu_{jm}}. \quad (9)$$

The factor $\Phi(\phi_m)$ is unity if $\phi_m > 0$ or $K_m Q_m > 1$, and zero otherwise, where ϕ_m denotes the mineral volume fraction. The sign of the rate is positive for precipitation and negative for dissolution and vanishes at equilibrium when $K_m Q_m = 1$.

- Chemical reactions included in PTRAN involve homogeneous and heterogeneous reaction between aqueous species and minerals which can be written in the general forms

$$\sum_j \nu_{ji} \mathcal{A}_j \rightleftharpoons \mathcal{A}_i, \quad (10)$$

$$\sum_j \nu_{jm} \mathcal{A}_j \rightleftharpoons \mathcal{M}_m, \quad (11)$$

respectively, where the set of species $\{\mathcal{A}_j\}$ refer to a set of primary or basis species in terms of which all other species are written, $\mathcal{A}_i$ denotes an aqueous complex referred to as a secondary species, and $\mathcal{M}_m$ refers to a mineral.

- The corresponding thermodynamic equilibrium constants K_i, K_m, and reaction stoichiometric coefficients ν_{ji}, ν_{jm} are derived from an extensive database for aqueous species, gases, and minerals.
- Partitioning CO_2 between H_2O and supercritical CO_2 is accomplished with the reaction

$$CO_{2(aq)} \rightleftharpoons CO_{2(g)}, \quad (12)$$

where the subscript (g) refers to the supercritical phase and (aq) to the aqueous phase. Other reactions not include above that may also significantly impact CO_2 sequestration are ion exchange and surface complexation reactions.

- Examples of Eqs.(10) and (11) for an aqueous fluid reacting with calcite consist of the following reaction network

$$CO_2 - H^+ + H_2O \rightleftharpoons HCO_3^-, \quad (13a)$$

$$CO_2 - 2H^+ + H_2O \rightleftharpoons CO_3^{2-}, \quad (13b)$$

$$Ca^{2+} + CO_2 - H^+ + H_2O \rightleftharpoons CaHCO_3^+, \quad (13c)$$

$$Ca^{2+} + CO_2 - 2H^+ + H_2O \rightleftharpoons CaCO_{3(aq)}, \quad (13d)$$

$$Ca^{2+} + CO_2 - 2H^+ + H_2O \rightleftharpoons CaCO_{3(s)}, \quad (13e)$$

described by the 4 primary species: Ca^{2+}, H^+, H_2O, and CO_2. The first four reactions involve only aqueous species and are referred to as homogeneous reactions. These reactions are considered to be sufficiently fast that local chemical equilibrium applies. The remaining reaction involves the solid phase calcite and thus is referred to as a heterogeneous reaction.

3.1 Coupling PFLOW and PTRAN

- The routines PFLOW and PTRAN are solved sequentially with an option to iterate between the PFLOW and PTRAN solutions until a fully consistent solution is obtained.
- Generally PTRAN requires smaller time steps than PFLOW and therefore it is necessary to interpolate field variables passed from PFLOW to PTRAN at the desired time. A linear interpolation relation is used to obtain pressure, temperature, saturation, and Darcy velocities of the fluid phases at intermediate times between two PFLOW time steps t_1, t_2, using a relation of the form of the form

$$\mathcal{F}(t) = \frac{t - t_1}{t_2 - t_1}\mathcal{F}_2 + \frac{t_2 - t}{t_2 - t_1}\mathcal{F}_1, \quad (14)$$

for $t_1 \le t \le t_2$, for field variable $\mathcal{F}$.

- To account for changes in porosity and permeability due to mineral reactions, PTRAN is used to calculate an updated porosity over a time step Δt from the relation

$$\phi(\boldsymbol{r}, t + \Delta t) = \phi(\boldsymbol{r}, t) - \Delta t \sum_m \overline{V}_m I_m(\boldsymbol{r}, t + \Delta t), \quad (15)$$

and the revised porosity is passed back to PFLOW. Permeability is derived from porosity through a power law or other phenomenological relation.

- Future implementations will explore independent grid hierarchies for PFLOW and PTRAN, as well as fully coupled schemes.

4. Parallel Implementation

- PFLOTRAN is written from the ground up to run on massively parallel computer architectures (Hammond et al., 2005).
- Parallelization is implemented through the PETSc parallel library developed at Argonne National Laboratory (Balay et al., 1997).
  - PETSc provides a user friendly set of routines for solving systems of nonlinear equations in parallel using domain decomposition [Figure 5(a)].
  - This includes parallel solvers and preconditioners, parallel construction of the Jacobian matrix and residual function, and seamless message passing, which together provide a high parallel efficiency.
  - PETSc (latest version 2.3.2) has achieved a high level of maturity that allows rapid development with efficient parallel implementation for solving systems of non-linear partial differential equations.
- PFLOTRAN makes use of object-oriented features in FORTRAN 90 and is essentially platform independent, running on any machine that PETSc runs on. This includes laptop computers, workstations, and massively parallel high performance computing facilities.

Flow of Control for PDE Solution

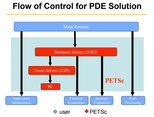

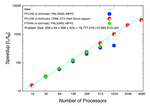

Figure 5: *PETSc provides message passing capabilities, solvers and preconditions for parallel computing (left). The user supplies the residual function and Jacobian. Performance of PFLOW and PTRAN (right) running a single phase thermo-hydrologic benchmark problem on a* $256 \times 64 \times 256$ *grid with three and four degrees of freedom per node, respectively (approximately 12.6 and 16.8 million degrees of freedom total).*

Sample parallel strong scaling is shown in Figure 5(b) for a modest sized problem running on MPP2 at PNNL/EMSL and Jaguar at ORNL (Mills et al., 2005). The benchmark was run on both the MPP2 cluster at PNNL/EMSL, a cluster of 1960 1.5 GHz Itanium 2 processors with Quadrics QsNetII interconnect, and Jaguar, the 5294 Opteron processor Cray XT3 at ORNL/NCCS. PFLOW scales quite well on both machines, bottoming out at around 1024 processors on MPP2, and scaling exceptionally well on Jaguar, displaying linear speedup all the way up to 2048 processors, and still displaying good speedup when going from there to 4096 processors. PTRAN scales similarly, which is not surprising because its computational structure is nearly identical to that of PFLOW. PFLOTRAN has been used to model CO_2 sequestration (Lu and Lichtner, 2005; Lu et al., 2005), and radionuclide transport at the Nevada Test Site (Lichtner and Wolfsberg, 2004).

- Multi-scale processes are based on a multiple interacting continuum formulation (Lichtner, 2000):
  - Primary continuum:

$$\frac{\partial}{\partial t}\epsilon_\alpha \varphi_\alpha \Psi_j^\alpha + \nabla\cdot\epsilon_\alpha \boldsymbol{\Omega}_j^\alpha = \sum_\beta A_{\beta\alpha}\Omega_j^{\alpha\beta} - \epsilon_\alpha \sum_s \nu_{js} A_s^\alpha I_s^\alpha \quad (16)$$

  - Secondary (sub-grid scale) continuum:

$$\frac{\partial}{\partial t}\varphi_\beta \Psi_j^\beta + \nabla\cdot\boldsymbol{\Omega}_j^\beta = -\sum_s \nu_{js} A_s^\beta I_s^\beta \quad (17)$$

  - Coupling:

$$C_j^\beta(r = r_\beta, t; \boldsymbol{r}) = C_j^\alpha(\boldsymbol{r}, t), \quad \Omega_j^{\alpha\beta} = -\varphi_\beta D_\beta \boldsymbol{n}_\beta \cdot \nabla \Psi_j^\beta \quad (18)$$

- Parallelization of multi-scale sub-grid scale model:
  - Rigorously decouple primary and sub-grid scale equations over a Newton iteration (step size in linear case)
  - Solve Sequence:
    - ➞ Eliminate sub-grid scale boundary concentration from primary continuum equation (forward "embarrassingly" parallel solve)
    - ➞ Solve primary equations in parallel using domain decomposition
    - ➞ Obtain sub-grid scale concentration (backward "embarrassingly" parallel solve)
  - The primary continuum residual is given by

$$R_{jn}^\alpha = \frac{(\epsilon_\alpha \varphi_\alpha \Psi_{jn}^\alpha)_{t+\Delta t} - (\epsilon_\alpha \varphi_\alpha \Psi_{jn}^\alpha)_t}{\Delta t} V_n + \sum_{n'} \Omega_{jnn'}^\alpha A_{nn'} + V_n \sum_s \nu_{js} I_{sn}^\alpha + \sum_\beta \epsilon_{jn}^{\beta n}\left(\Psi_{jn}^\alpha - \Psi_{jM}^{\beta n}\right) \quad (19)$$

where $\Psi_{jM}^{\beta n}$ is the coupling to the sub-grid scale model.

  - The sub-grid scale secondary continua equations are:

$$\boldsymbol{\alpha}_1 \delta\boldsymbol{\Psi}_1^\beta + \boldsymbol{\gamma}_1 \delta\boldsymbol{\Psi}_2^\beta = \boldsymbol{r}_1 \quad (20a)$$

$$\boldsymbol{\beta}_2 \delta\boldsymbol{\Psi}_1^\beta + \boldsymbol{\alpha}_2 \delta\boldsymbol{\Psi}_2^\beta + \boldsymbol{\gamma}_2 \delta\boldsymbol{\Psi}_3^\beta = \boldsymbol{r}_2 \quad (20b)$$

$$\cdots$$

$$\boldsymbol{\beta}_m \delta\boldsymbol{\Psi}_{m-1}^\beta + \boldsymbol{\alpha}_m \delta\boldsymbol{\Psi}_m^\beta + \boldsymbol{\gamma}_m \delta\boldsymbol{\Psi}_{m+1}^\beta = \boldsymbol{r}_m \quad (20c)$$

$$\cdots$$

$$\boldsymbol{\beta}_{M-1} \delta\boldsymbol{\Psi}_{M-2}^\beta + \boldsymbol{\alpha}_{M-1} \delta\boldsymbol{\Psi}_{M-1}^\beta + \boldsymbol{\gamma}_{M-1} \delta\boldsymbol{\Psi}_M^\beta = \boldsymbol{r}_{M-1} \quad (20d)$$

$$\boldsymbol{\beta}_M \delta\boldsymbol{\Psi}_{M-1}^\beta + \boldsymbol{\alpha}_M \delta\boldsymbol{\Psi}_M^\beta = \boldsymbol{r}_M(\Psi_m^\alpha) \quad (20e)$$

where Ψ_m^α is the coupling to the primary continuum.

5. Applications

A number of applications will be investigated that require high performance computing. These include the Hanford 300 Area, CO_2 sequestration, and radionuclide migration at the Nevada Test Site.

5.1 Hanford 300 Area

- Uranium concentrations in the groundwater of the Hanford 300 Area continue to exceed the drinking water standard in spite of engineering calculations that predicted cleanup by natural attenuation.
- Laboratory experiments indicate that a key process in the uranium persistence is the presence of pore structures that limit mass transfer (Zachara et al., 2005).
- The accurate characterization of pore scale effects and effective sub-grid parameterizations would provide scientifically defensible decision making for engineered solutions.
- We will apply PFLOTRAN to a site wide model of U(VI) migration at the Hanford 300 Area. Our analysis will include:
  - surface complexation and ion exchange reactions, and kinetic phenomena caused by intra-grain diffusion and precipitation/dissolution of U(VI) solid phases to account for the observed slow leaching of U(VI) from the source zone.
  - Both transport in the vadose zone where the U(VI) source is located and saturated groundwater flow to the Columbia River will be taken into account.
  - An important consideration in a robust model for the 300 Area is remobilization of U(VI) as the rising and falling stage of the Columbia River causes river water to mix with ambient groundwater in the vadose zone. To adequately model this system will require taking into account changes in the river stage on a daily basis. We will using AMR to track this transient behavior induced by river stage fluctuations.

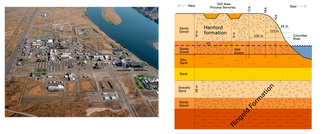

Figure 6: *An aerial view of the Hanford 300 Area is shown on the left with a stratigraphic cross section shown on the right.*

5.2 Subsurface CO_2 Sequestration

- We will apply PFLOTRAN with its newly developed AMR capability to model the effects of CO_2 sequestration in a subsurface reservoir.
- We will include the presence of an oil phase and four phase liquid-gas-aqueous-oil system to describe dissipation of the supercritical CO_2 phase and escape of CO_2 to the surface.
- The addition of compositional oil will be added to the code using a generic multiphase capability.
- Simulations will be conducted first for a porous medium that is homogeneous at all scales so that the complications of upscaling issues can be avoided. This will enable us to test the AMR algorithm's ability to track reaction fronts and changes in phase boundaries separately.
- Next, a consistent set of hierarchical permeability and dispersivity fields will be developed at different scales using various upscaling algorithms, including multilevel techniques.

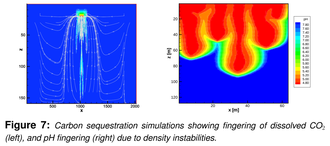

Figure 7: *Carbon sequestration simulations showing fingering of dissolved* CO_2 *(left), and pH fingering (right) due to density instabilities.*

- A feature of interest will be resolution of fingering in 3D simulations produced from buoyancy effects caused by an increase in density as supercritical CO_2 dissolves into the formation brine. Finger widths may be on the order of meters or smaller depending on the properties of the reservoir.
- Working with LANL DOE-FE Regional Partnerships on CO_2 sequestration we will identify a field site and apply PFLOTRAN to model a 3D field CO_2 injection scenario. LANL is part of two regional partnerships that are planning four field experiments between them, ranging in size from several thousand tons to millions of tons and ranging in lithology from sandstones to carbonates to basalts. Our proposed work in these partnerships includes collection of data and observations that would be excellent for a computational study on reactive flow in complex geologic environments.
- We expect the accuracy of our predictive capability to increase as more data becomes available for the various multiphase constitutive relations needed in simulations. Through the versatile and modular structure of PFLOTRAN, it will be relatively easy to add new constitutive relations as they become available.

6. Conclusion

PFLOTRAN is being developed to provide next-generation capabilities in modeling reactive flows in porous media.

- Features:
  - modular structure based on F90 and C++
  - multiscale processes
  - AMR
  - unstructured grids
  - upscaling material properties
  - multiphase, multicomponent reactions
- Applications:
  - Hanford 300 Area
  - CO_2 sequestration
  - Nevada Test Site
  - Shale Hills PA, ...

Acknowledgments This work is partially supported by a SciDAC-2 award under Contract No. DE-AC52-06NA25396 from the U.S. Department of Energy.

7. References

Balay, S., W.D. Gropp, L.C. McInnes and B.F. Smith (1997) Efficient Management of Parallelism in Object Oriented Numerical Software Libraries, Modern Software Tools in Scientific Computing, Ed. E. Arge, A. M. Bruaset and H. P. Langtangen, 163-202, Birkhauser Press.

Hammond, G., Valocchi, V., Lichtner, P.C. (2005) Application of Jacobian-free Newton-Krylov with physics-based preconditioning to biogeochemical transport, Advances in Water Resources, 28, 359–376.

Hornung, R.D. and J.A. Trangenstein (1997) Adaptive mesh refinement and multilevel iteration for flow in porous media. J. Comp. Phys. 136, 522–545.

Knepley, M.G. and D.A. Karpeev (2005) Flexible Representation of Computational Meshes, Argonne National Laboratory, ANL/MCS-P1295-1005. Submitted to TOMS.

Lichtner, P.C. (2000) Critique of Dual Continuum Formulations of Multicomponent Reactive Transport in Fractured Porous Media, Dynamics of Fluids in Fractured Rock. Geophys. Monograph, 122, 281–298.

Lichtner, P.C. and Q. Kang (2007) Upscaling Pore-Scale Reactive Transport Equations using a Multi-Scale Continuum Formulation, Water Resources Research, in press.

Lichtner, P.C. and A. Wollsberg (2004) Modeling Thermal-Hydrologic-Chemical (THC) Coupled Processes with Application to Underground Nuclear Tests at the Nevada Test Site: A "Grand Challenge" Supercomputing Problem, MOU Workshop: Conceptual Model Development for Subsurface Reactive Transport Modeling of Inorganic Contaminants, Radionuclides, and Nutrients, April 20-22, Albuquerque, NM, Los Alamos National Laboratory report LA-UR-04-1826.

Lichtner, P.C., C. I. Steefel, and E. H. Oelkers (1996) Reactive transport in porous media. Reviews in Mineralogy, 34, 438.

Lu, C., P.C. Lichtner, I.N. Tsimpanogiannis, and R.T. Mills (2005) Parametric study of CO_2 sequestration in geologic media using the massively parallel computer code PFLOTRAN, AGU, San Francisco.

Lu C., P.C. Lichtner (2005) PFLOTRAN: Massively Parallel 3-D Simulator for CO_2 Sequestration in Geologic Media, Fourth Annual Conference on Carbon Capture and Sequestration DOE/NETL.

MacLachlan, S.P., and J.D. Moulton (2006) Multilevel upscaling through variational coarsening. Water Resour. Res., 42, W02418, doi10.1029/2005WR003940

Mills, R.T., C. Lu, and P.C. Lichtner (2005) PFLOTRAN: A massively parallel simulator for reactive flows in geologic media, SC2005.

Moulton, J.D., J.E. Dendy, J.M. Hyman (1998) The black box multigrid numerical homogenization algorithm. J. Comput. Phys., 142, 80–108.

Pernice, M. and B. Philip (2006) Solution of Equilibrium Radiation Diffusion Problems Using Implicit Adaptive Mesh Refinement, SIAM, 27(5), 1709–1726.

Wang, Y., R. Reddy, R. Gomez, J. Lim, S. Sanielevici, J. Ray, J. Sutherland, and J. Chen (2004) A general approach to creating FORTRAN interface for C++ application libraries, SciDAC Scientific Application Pilot Programs (SAPP), Proceedings of the International Conference on High Performance Computing and Applications, August 810, 2004, Shanghai, P.R. China.

Zachara J.M., J.A. Davis, C. Liu, J.P. McKinley, N. Qafoku, D.M. Wellman, and S.B. Yabusaki (2005) Uranium Geochemistry in Vadose Zone and Aquifer Sediments from the 300 Area Uranium Plume. PNNL-15121, Pacific Northwest National Laboratory, Richland, Washington.